NANO LETTERS

Letter

pubs.acs.org/NanoLett

Atomistic Design of CdSe/CdS Core−Shell Quantum Dots with Suppressed Auger Recombination

Ankit Jain,[†] Oleksandr Voznyy,[†] Sjoerd Hoogland,[†] Marek Korkusinski,[‡] Pawel Hawrylak,[§] and Edward H. Sargent*[,†]

[†]Department of Electrical and Computer Engineering, University of Toronto, 10 King's College Road, Toronto, Ontario M5S 3G4, Canada

[‡]National Research Council of Canada, Ottawa, Ontario K1A 0R6, Canada

[§]Department of Physics, University of Ottawa, Ottawa, Ontario K1N 6N5, Canada

Supporting Information

ABSTRACT: We design quasi-type-II CdSe/CdS core−shell colloidal quantum dots (CQDs) exhibiting a suppressed Auger recombination rate. We do so using fully atomistic tight-binding wave functions and microscopic Coulomb interactions. The recombination rate as a function of the core and shell size and shape is tested against experiments. Because of a higher density of deep hole states and stronger hole confinement, Auger recombination is found to be up to six times faster for positive trions compared to negative ones in 4 nm core/10 nm shell CQDs. Soft-confinement at the interface results in weak suppression of Auger recombination compared to same-bandgap sharp-interface CQDs. We find that the suppression is due to increased volume of the core resulting in delocalization of the wave functions, rather than due to soft-confinement itself. We show that our results are consistent with previous effective mass models with the same system parameters. Increasing the dot volume remains the most efficient way to suppress Auger recombination. We predict that a 4-fold suppression of Auger recombination can be achieved in 10 nm CQDs by increasing the core volume by using rodlike cores embedded in thick shells.

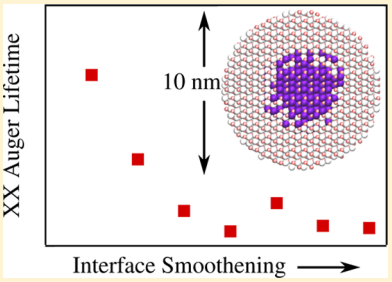

KEYWORDS: *Auger recombination, atomistic simulations, core−shell quantum dots, interface grading, tight-binding, CdSe/CdS*

Semiconductor CQDs have been a focus of intense research in the past two decades for applications ranging from biological fluorescence tagging[1,2] and photovoltaics[3−5] to light-emitting diodes[6−8] and lasers.[9,10] Among many interesting properties of CQDs are solution processability, size-tunable bandgap, and high-photoluminescence quantum yield (PLQY).[11]

While these properties of CQDs have resulted in major advances in CQD-based devices, it remains important to reduce the unwanted nonradiative losses in CQDs.[5,12,13]

Auger recombination is a major nonradiative loss in CQDs under high excitation intensity, where a photoexcited electron−hole pair transfers its energy nonradiatively to another carrier.[14] In contrast to bulk semiconductors, where Auger recombination is inefficient, the process is significantly enhanced in CQDs due to relaxation of the momentum conservation requirement and increased Coulomb interactions.[12,15−20] Auger recombination is believed to be the cause of reduced PLQY at high pump intensities,[21] low external quantum efficiency of light-emitting diodes under high bias,[8] loss of energy in the form of heat,[8] and fluorescence intermittency (blinking) often observed in CQDs.[22,23]

Grading, that is, a smooth core−shell interface, has been explored as a means to mitigate Auger recombination. Using the effective mass approximation (EMA), Cragg and Efros[24] found more than a 3 orders of magnitude reduction in the Auger recombination rate in graded-interface CQDs. In experiments, the effect of grading was less conclusive with findings varying from study to study.[25−28] Other approaches such as thick shell type-II/quasi-type-II core−shell CQDs[29−32] have also been proposed to suppress Auger recombination; however, a clear design of CQDs with substantial elimination of Auger recombination losses has yet to emerge.[3,33] The complex dynamics of multiexcitons in CQDs make these phenomena difficult to measure experimentally and model computationally.[15,34,35]

In this Letter, we use atomistic tight-binding wave functions[36,37] to obtain realistic Coulomb matrix elements, allowing us to determine paths to reducing Auger recombination in realistic-size CQDs with up to ∼11 nm diameter. We include ∼22 000 atoms and ∼100 000 atomic orbitals per CQD state, capturing thereby the complexities of the conduction band and especially the valence band. We study the effect of shell thickness, interface softening (grading), core size, and valence versus conduction band structure effects on the Auger recombination rates in negatively charged (X^- trion), positively

Received: July 22, 2016
Revised: September 19, 2016
Published: September 26, 2016

DOI: 10.1021/acs.nanolett.6b03059
Nano Lett. 2016, 16, 6491−6496

charged (X^+ trion), and biexciton (XX) in quasi-type-II CdSe/CdS wurtzite core−shell CQDs (Figure 1a−c). We find that

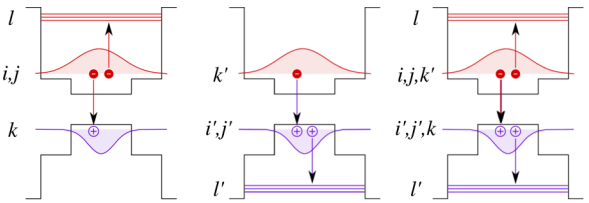

Figure 1. Auger recombination channels considered in this work. (a) Negative trion (X^-), (b) positive trion (X^+), and (c) biexciton (XX). The electron−hole recombination energy in biexciton can be transferred to the second electron (four pathways) or to the second hole (four pathways).

interface grading allows increase in the core volume without affecting the bandgap. This in turn results in more delocalized wave functions and thus weaker overlaps and reduced Auger recombination rates. The latter is consistent with EMA observations by Cragg and Efros[24] but without the need to invoke the role of interface softness in defining the high-frequency components of the wave functions. Additionally, we find that interface alloying disorder (not accessible in EMA) enhances the Auger recombination rate, counteracting the effect of increasing core volume. We further show that the Auger recombination rate can be decreased 4-fold by changing the core shape from spherical to ellipsoidal. To the best of our knowledge, this is the first study that uses fully atomistic simulations to investigate Auger recombination in realistic size core−shell CQDs.

We consider three different types of Auger recombination processes in this study, namely, negative trion (X^-), positive trion (X^-), and biexcition (XX) (Figure 1a−c). We calculate Auger recombination rate for trions by considering all transitions from the lowest-energy initial spin-degenerate single-particle configurations $|ij\rangle$ to final spin-degenerate configurations $|kl\rangle$ with either electron or hole excited, in the lowest order in Coulomb interactions using the Fermi golden rule[38]

$$\frac{1}{\tau_A} \equiv \frac{1}{\tau_k^{ij}} = \sum_l \frac{2\pi}{\hbar} |\langle kl|V_c|ij\rangle|^2 \, \delta(E_i + E_j - E_k - E_l) \quad (1)$$

where τ_A is the Auger lifetime, $\hbar$ is the reduced Planck constant, $\langle kl|V_c|ij\rangle$ is the Coulomb matrix element between single particle electronic states $|i\rangle$, $|j\rangle$, $|k\rangle$, $|l\rangle$ with energies E_i, E_j, E_k, E_l, and $\delta(E_i + E_j - E_k - E_l)$ δ-function ensures the energy conservation. The summation in eq 1 is over all deep electronic states which satisfy energy conservation. For biexcitons, we calculate the Auger recombination rate using the statistical averaging as $\tau_{XX}^{-1} = 2(\tau_{X^-}^{-1} + \tau_{X^+}^{-1})$,[39] where τ_{XX}, τ_{X^-}, and τ_{X^+} are Auger recombination lifetimes in biexciton, negative trion, and positive trion. (For Auger rates between true correlated biexcitonic and excitonic states and a full treatment of Coulomb interactions, see ref 40.)

We approximated the delta function in eq 1 using a Lorentzian of 30 meV width[41] and obtained all deep single particle states within 100 meV of the required energy level explicitly by diagonalizing the tight-binding Hamiltonian, calculated using QNANO,[42] using the Lanczos algorithm as implemented in the eigenvalue library FEAST.[43] In our model, single particle state calculations are carried out in the linear combination of atomic orbitals basis and we parametrized our tight-binding Hamiltonian using on-site orbital energies, spin−orbit coupling constants, and hopping matrix elements connecting orbitals of neighboring atoms.[44] We considered spin-degenerate $sp_3d_5s^*$ orbitals and fit our tight-binding parameters to the bulk bandstructures of the core and shell materials predicted using density functional theory. Further, we included Coulomb interactions, unscreened for on-site Coulomb matrix elements and screened with the bulk dielectric constant of CdSe for off-site interactions.[45] We note that we considered only bandedge trions and we did not take strain into account in this study. Further details regarding our tight-binding Hamiltonian can be found in refs 40 and 44.

The validity of our calculations is tested by comparing with the experimentally measured Auger recombination lifetimes for negative and positive trions, and their scaling with CQD size. As can be seen from Table S1, our calculations accurately predict the Auger recombination lifetimes in positive and negative trions in both core-only and core−shell CQDs over the range of dot sizes considered.

We first investigate the effect of shell thickness on Auger recombination lifetimes in core−shell CQDs (Figure 2a). We fixed the core diameter at 4 nm and varied the total CQD diameter from 4 to 10.5 nm. With an increase in shell thickness, Auger recombination lifetimes show three distinct features: (i) lifetimes are notably longer for negative trions than for positive trions (except for smaller CQDs), (ii) lifetimes change nonmonotonically with shell thickness, and (iii) overall Auger recombination lifetimes are longer in thicker-shell CQDs. To understand the origin of these features, we report the density of states (DOS) and wave functions in Figure 2b,c−f.

We find that the density of deep conduction band states is up to four times lower than the density of deep valence band states. This, along with stronger hole confinement, results in slower Auger recombination of negative trions as compared to positive trions. With an increase in shell thickness, the total CQD volume increases and the deep conduction and valence band states become more delocalized, resulting in weaker overlap with the initial bandedge states and correspondingly a slowing in Auger recombination. For core-only CQDs (inset of Figure 2a), the Auger recombination lifetimes scale with CQD diameter, d, as $d^{6.2}$ for biexcitons (5.4 and 7.0 for negative and positive trions, respectively), which is within the range of experimentally measured exponents of 5.6−6.3 by Kobayashi et al.[46] We discuss the comparison of our shell-thickness dependent Auger lifetimes against the experimentally measured values of Garcia-Santamaria et al.[25] in Figure S2 in the SI.

Our predicted nonmonotonic variation of Auger recombination lifetimes with shell thickness agrees qualitatively with a recent theoretical study by Efros et al.[24,32] Using the eight-band **k·p** method, the authors showed that the Auger recombination rate can vary over an order of magnitude for a shell thickness fluctuation within 1 nm.[32] In our calculations, however, these variations are within a factor of 3. The main reason for this difference resides in the number and the symmetry of the deep states, which differ between atomistic and EMA calculations.[47] A higher density of states and Lorentzian broadening allow us to avoid the vanishing of the Auger rates for specific dot sizes observed in EMA[24] when the initial and final configurations are not in resonance.

The predicted oscillations in Auger lifetimes in Figure 2a originate from a broad distribution of Coulomb element values

DOI: 10.1021/acs.nanolett.6b03059
Nano Lett. 2016, 16, 6491−6496

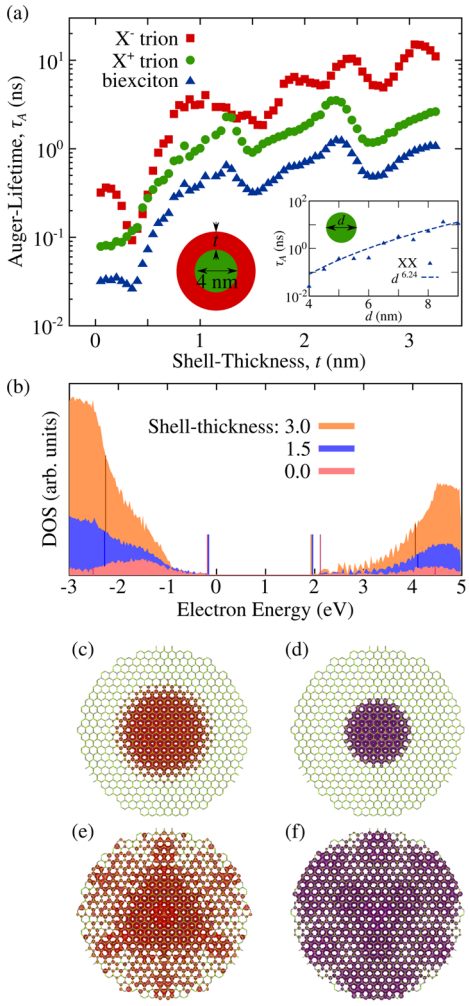

Figure 2. The effect of shell thickness on Auger recombination. (a) Predicted Auger recombination lifetimes for negative, positive trions, and biexcitons as a function of shell thickness in core−shell quasi-type-II CQDs. (b) Density of states in core-only, 1.5 nm, and 3.0 nm thick-shell CQDs. Electron charge density for single particle states at the conduction bandedge (c), at the valence bandedge (d), deep in conduction band (e), and deep in valence band (f). The inset in (a) shows the variation of biexciton Auger recombination lifetimes with diameter in core-only CQDs.

that couple the bandedge states to deep states. As seen in the **k**·**p** model,[32] high-frequency states that couple well to the bandedge states appear periodically across the relevant energy range. Scanning through different shell thickness brings these states in and out of resonance. As such, the distribution of Coulomb elements is representative of a single CQD and would be completely smoothened out in an ensemble possessing realistic variations in size and shape.

Next, we investigate the effect of mixing at the interface which was suggested by previous EMA model to suppress the Auger recombination.[24] We fix the core size at 4 nm in a 9 nm core−shell CQD. We varied the intermixing fraction (smoothness) by swapping the desired fraction of atoms within 0.5 nm on both sides of the interface. When we increase the interface mixing, all Auger recombination lifetimes shorten by a factor of 2, quickly reaching saturation after 20% mix fraction (Figure 3).

This apparent contradiction with EMA findings[24] can be resolved by looking at wave function localization volumes. Interface grading results in effective narrowing of the potential

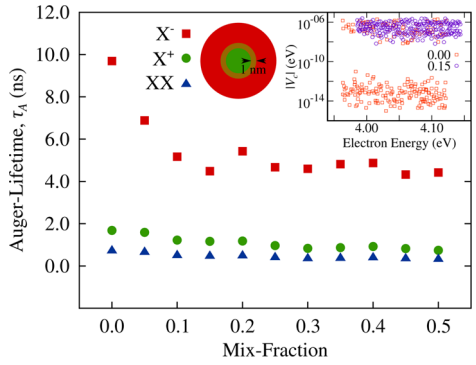

Figure 3. Effect of interface grading on Auger recombination. Predicted Auger recombination lifetimes for negative and positive trions and biexcitons as a function of interface mixing for quasi-type-II core−shell CQDs. (Inset) Change in Coulomb matrix elements upon introducing a mixture of 15% in negatively charged CQD, as a function of deep-electron energy. Alloying at the interface breaks the system symmetry and eliminates zero-valued Coulomb matrix elements observed in sharp interface case.

well, leading to more strongly localized wave functions (see SI Figure S3a) and their stronger overlap and faster Auger rate through eq 1. However, the EMA model in ref 24 was constructed for a much shallower confinement potential (300 meV), representative of epitaxial QDs but not colloidal QDs. In this case, confinement energy is comparable to the potential well depth. Graded interface produces higher confinement energy, which pushes the wave function out of the potential well (see SI Figure S3b). The wave function is more delocalized in case of soft potential and Auger rate is smaller, that is, the trend is reversed compared to deep potential well relevant for CQDs.

An additional factor that speeds Auger recombination in case of soft confinement is revealed when one investigates the Coulomb matrix elements (inset in Figure 3). For a sharp interface, about one-third of the Coulomb matrix elements are zero. We noticed such behavior previously[40] and tentatively ascribed it to poor overlap of the corelike and surface-like deep states. However, in this work the nanocrystals are large enough that we can see clearly that the final states are not surface-derived. Instead, the zero matrix elements can be ascribed to the symmetry of the deep state with its high-frequency oscillations that integrate to zero when overlapped with the initial core state, similar to EMA findings.[32] With alloying at the interface, the CQDs become less symmetric, resulting in the change of the deep states shape. As a result, all Coulomb matrix elements become nonzero, resulting in a faster overall Auger recombination.

We verified the strength of this effect by comparing two kinds of soft-confinement, one with alloyed interface (atomic disorder) and another with averaged interface (virtual crystal approximation) comparable to EMA models (Figure 4b,c). Comparison of artificially averaged versus sharp interface (Figure 4a,c) shows nearly no Auger recombination suppression because the degree of softening introduced here (ν = 20 for soft versus ν = 60 for sharp interface in Cragg and Efros notation) is significantly smaller than that discussed by Cragg and Efros ($\nu = \infty$ vs ν = 2).[24] Atomic alloying results in ∼2× faster Auger rates than artificially averaged interface (Figure 4b,c).

Experimental studies aimed at verifying the effect of soft confinement on Auger rates reported varying results. Some

DOI: 10.1021/acs.nanolett.6b03059
Nano Lett. 2016, 16, 6491−6496

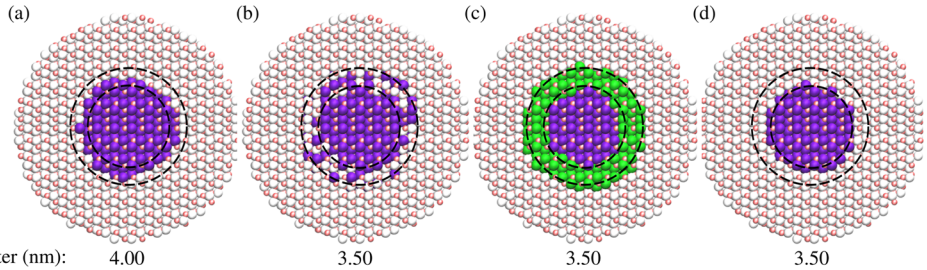

	(a)	(b)	(c)	(d)
Core-diameter (nm):	4.00	3.50	3.50	3.50
Interface-width (nm):	-	1.00	1.00	-
E_g (eV):	2.10	2.15	2.15	2.15
τ_{X^-} (ns):	9.70	4.42	10.45	2.36
τ_{X^+} (ns):	1.68	0.74	1.36	0.30
τ_{XX} (ns):	0.72	0.32	0.60	0.13

Figure 4. Effect of soft confinement adjusted for bandgap variations. Electronic bandgap, negative trion, positive trion, and biexciton Auger lifetimes in quasi type-II core−shell CQDs with (a) 4.0 nm core, (b) soft confinement achieved through alloyed interface (atomic disorder), (c) soft-confinement achieved through averaged (virtual crystal approximation) interface, and (d) 3.5 nm core. The dashed circles are guides to the eye representing 3.5 and 4.5 nm diameters.

studies demonstrated suppressed Auger recombination,[26,27] while others argued that the effect is not related to soft confinement.[28] To investigate the origin of these disparate findings, we compared various CQDs with different core sizes and degrees of soft confinement (Figure 4). As mentioned above, interface softening leads to a narrowing of the core potential and increase of the bandgap due to ensuing stronger confinement. To compensate for this effect we add to our comparison a model with a 3.5 nm core and sharp interface (Figure 4d) that achieves the same bandgap as the soft-confined model.

In comparing sharp and soft interfaces while maintaining the same bandgap (Figure 4b,d), we find that a softened interface results in longer Auger recombination lifetime. The effect is noticeable despite the disorder-induced enhancement of Auger recombination discussed above. In the case of a comparison for nominally constant core volumes (Figure 4a,b), however, the softer interface results in faster Auger recombination. These findings show that Auger recombination suppression is a result of volume scaling of lifetimes and not of the softness itself.

Distinguishing the bandgap versus core volume comparisons allows us to reconcile the seemingly contradictory experimental findings. Experimental reports demonstrating Auger recombination suppression[26,27] in fact increased the core volume, as can be seen from the shift in absorption wavelength. Recently, Beyler et al.[28] measured a sample-averaged biexciton quantum yield using solution-phase photon correlation. Consistent with our findings, the difference between the sharp and soft interfaces was found to be negligible, provided that the interface does not introduce any defects.

In light of our finding that the increase in volume has the strongest effect on Auger recombination (Figure 2a) in CQDs, we next try to increase the core volume. For this, we used ricelike ellipsoidal cores where the smaller diameter of an ellipsoid is fixed at 4 nm and the length of the ellipsoid is varied to tune the degree of hole delocalization. Our predicted values of trion and biexciton Auger recombination lifetimes for these CQDs as a function of core-length are presented in Figure 5. Upon increasing the core length from 4 to 8 nm, the positive trion and biexciton Auger recombination lifetimes increase by more than a factor of 6 and 4, respectively.

According to eq 1, the Auger recombination rate is proportional to the strength of Coulomb matrix elements and the density of final states. We vary the aspect ratio of the core

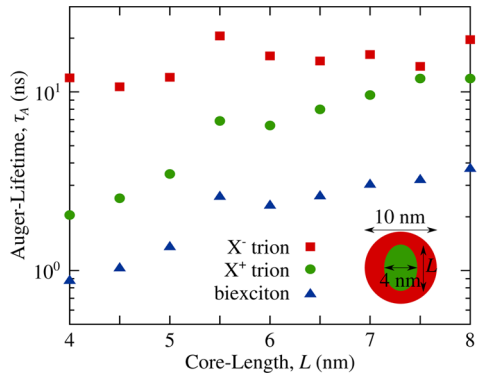

Figure 5. Core-shape-dependent Auger recombination lifetimes. Predicted Auger recombination lifetimes for negative and positive trions and biexcitons as a function of ellipsoid core length for CdSe/CdS core−shell CQDs. Negative trion, positive trion, and biexciton Auger recombination lifetimes increase by factors of 2, 6, and 4 in increasing the core-length from 4 to 8 nm.

and keep the total CQD volume the same. Irrespective of the core length, therefore, the density of the final deep states remains unchanged. This suggests that a decrease in Coulomb matrix elements is the main cause of reduced Auger recombination upon increasing the core length.

In summary, we used fully atomistic tight-binding calculations to design quasi-type-II CdSe/CdS core−shell CQDs with reduced Auger recombination. We explicitly calculated all single-particle states by diagonalizing the tight-binding Hamiltonian that is fit to bulk bandstructures. We find that Auger recombination through the positive trion is up to six times faster than through the negative trion in a 4 nm core/10 nm shell spherical-core CQDs due to higher density of deep valence band states and stronger confinement of the hole. Larger cores and thicker shells efficiently suppress Auger recombination. Similarly, Auger recombination suppression upon softening of the core−shell interface is predominantly a result of the increased core volume, whereas the soft confinement itself has little effect.

We predict that a 4-fold suppression of Auger recombination can be achieved in 10 nm CQDs by increasing the core volume by using rodlike cores embedded in thick shells. We also showed that atomic disorder results in enhancement of Auger recombination due to relaxation of the symmetry-based

DOI: 10.1021/acs.nanolett.6b03059
Nano Lett. 2016, 16, 6491−6496

selection rules. Our study provides new design rules to suppress Auger recombination by using larger core and shell volume, a disorder-free interface, and negatively charged CQDs.

■ ASSOCIATED CONTENT

Supporting Information

The Supporting Information is available free of charge on the ACS Publications website at DOI: 10.1021/acs.nanolett.6b03059.

Comparison with experiments, EMA wave functions, and Lorentzian width convergence (PDF)

■ AUTHOR INFORMATION

Corresponding Author

*E-mail: ted.sargent@utoronto.ca.

Author Contributions

A.J. and O.V. contributed equally to this work.

Notes

The authors declare no competing financial interest.

■ ACKNOWLEDGMENTS

This research is supported in part by the Natural Sciences and Engineering Research Council (NSERC) of Canada, by the Ontario Research Fund Research Excellence Program, and by the IBM Canada Research and Development Center. A.J. is supported by the IBM Canada Research and Development Center through the Southern Ontario Smart Computing Innovation Platform (SOSCIP) postdoctoral fellowship. The SOSCIP consortium is funded by the Ontario Government and the Federal Economic Development Agency for Southern Ontario. Computations were performed on the GPC supercomputer at the SciNet HPC Consortium. SciNet is funded by the Canada Foundation for Innovation under the auspices of Compute Canada; the Government of Ontario; Ontario Research Fund - Research Excellence; and the University of Toronto. P.H. acknowledges support by the University of Ottawa Research Chair in Quantum Theory of Materials, Nanostructures and Devices.

■ REFERENCES

(1) Bruchez, M.; Moronne, M.; Gin, P.; Weiss, S.; Alivisatos, A. P. *Science* **1998**, *281*, 2013−2016.

(2) Biju, V.; Muraleedharan, D.; Nakayama, K.; Shinohara, Y.; Itoh, T.; Baba, Y.; Ishikawa, M. *Langmuir* **2007**, *23*, 10254−10261.

(3) Kobayashi, Y.; Udagawa, T.; Tamai, N. *Chem. Lett.* **2009**, *38*, 830−831.

(4) Beard, M. C.; Midgett, A. G.; Hanna, M. C.; Luther, J. M.; Hughes, B. K.; Nozik, A. J. *Nano Lett.* **2010**, *10*, 3019−3027.

(5) Semonin, O. E.; Luther, J. M.; Choi, S.; Chen, H.-Y.; Gao, J.; Nozik, A. J.; Beard, M. C. *Science* **2011**, *334*, 1530−1533.

(6) Colvin, V.; Schlamp, M.; Alivisatos, A. *Nature* **1994**, *370*, 354−357.

(7) Mashford, B. S.; Stevenson, M.; Popovic, Z.; Hamilton, C.; Zhou, Z.; Breen, C.; Steckel, J.; Bulovic, V.; Bawendi, M.; Coe-Sullivan, S. *Nat. Photonics* **2013**, *7*, 407−412.

(8) Bae, W. K.; Park, Y.-S.; Lim, J.; Lee, D.; Padilha, L. A.; McDaniel, H.; Robel, I.; Lee, C.; Pietryga, J. M.; Klimov, V. I. *Nat. Commun.* **2013**, *4*, 3661.

(9) Klimov, V.; Mikhailovsky, A.; Xu, S.; Malko, A.; Hollingsworth, J.; Leatherdale, C.; Eisler, H.-J.; Bawendi, M. *Science* **2000**, *290*, 314−317.

(10) Michler, P.; Imamoğlu, A.; Mason, M.; Carson, P.; Strouse, G.; Buratto, S. *Nature* **2000**, *406*, 968−970.

(11) Klimov, V. I. *Semiconductor and metal nanocrystals: synthesis and electronic and optical properties*; CRC Press: Boca Raton, FL, 2003.

(12) Klimov, V. I.; Mikhailovsky, A.; McBranch, D.; Leatherdale, C.; Bawendi, M. G. *Science* **2000**, *287*, 1011−1013.

(13) Achermann, M.; Bartko, A. P.; Hollingsworth, J. A.; Klimov, V. I. *Nat. Phys.* **2006**, *2*, 557−561.

(14) Landsberg, P. T. *Basic Properties of Semiconductors*; Elsevier: New York, 2013.

(15) Wang, L.-W.; Califano, M.; Zunger, A.; Franceschetti, A. *Phys. Rev. Lett.* **2003**, *91*, 056404.

(16) Pandey, A.; Guyot-Sionnest, P. *J. Chem. Phys.* **2007**, *127*, 111104.

(17) Pietryga, J. M.; Zhuravlev, K. K.; Whitehead, M.; Klimov, V. I.; Schaller, R. D. *Phys. Rev. Lett.* **2008**, *101*, 217401.

(18) Robel, I.; Gresback, R.; Kortshagen, U.; Schaller, R. D.; Klimov, V. I. *Phys. Rev. Lett.* **2009**, *102*, 177404.

(19) Jha, P. P.; Guyot-Sionnest, P. *ACS Nano* **2009**, *3*, 1011−1015.

(20) Klimov, V. I. *Annu. Rev. Condens. Matter Phys.* **2014**, *5*, 285−316.

(21) Shen, Y.; Mueller, G.; Watanabe, S.; Gardner, N.; Munkholm, A.; Krames, M. *Appl. Phys. Lett.* **2007**, *91*, 141101.

(22) Nirmal, M.; Dabbousi, B.; Bawendi, M.; Macklin, J.; Trautman, J.; Harris, T.; Brus, L. *Nature* **1996**, *383*, 802−804.

(23) Galland, C.; Ghosh, Y.; Steinbrück, A.; Sykora, M.; Hollingsworth, J. A.; Klimov, V. I.; Htoon, H. *Nature* **2011**, *479*, 203−207.

(24) Cragg, G. E.; Efros, A. L. *Nano Lett.* **2010**, *10*, 313−317.

(25) García-Santamaría, F.; Brovelli, S.; Viswanatha, R.; Hollingsworth, J. A.; Htoon, H.; Crooker, S. A.; Klimov, V. I. *Nano Lett.* **2011**, *11*, 687−693.

(26) Bae, W. K.; Padilha, L. A.; Park, Y.-S.; McDaniel, H.; Robel, I.; Pietryga, J. M.; Klimov, V. I. *ACS Nano* **2013**, *7*, 3411−3419.

(27) Park, Y.-S.; Bae, W. K.; Padilha, L. A.; Pietryga, J. M.; Klimov, V. I. *Nano Lett.* **2014**, *14*, 396−402.

(28) Beyler, A. P.; Bischof, T. S.; Cui, J.; Coropceanu, I.; Harris, D. K.; Bawendi, M. G. *Nano Lett.* **2014**, *14*, 6792−6798.

(29) Klimov, V. I.; Ivanov, S. A.; Nanda, J.; Achermann, M.; Bezel, I.; McGuire, J. A.; Piryatinski, A. *Nature* **2007**, *447*, 441−446.

(30) Saba, M.; Minniberger, S.; Quochi, F.; Roither, J.; Marceddu, M.; Gocalinska, A.; Kovalenko, M. V.; Talapin, D. V.; Heiss, W.; Mura, A. *Adv. Mater.* **2009**, *21*, 4942−4946.

(31) Vaxenburg, R.; Rodina, A.; Shabaev, A.; Lifshitz, E.; Efros, A. L. *Nano Lett.* **2015**, *15*, 2092−2098.

(32) Vaxenburg, R.; Rodina, A.; Lifshitz, E.; Efros, A. *Nano Lett.* **2016**, *16*, 2503−2511.

(33) Zavelani-Rossi, M.; Lupo, M. G.; Tassone, F.; Manna, L.; Lanzani, G. *Nano Lett.* **2010**, *10*, 3142−3150.

(34) Califano, M.; Zunger, A.; Franceschetti, A. *Appl. Phys. Lett.* **2004**, *84*, 2409−2411.

(35) Rabani, E.; Baer, R. *Nano Lett.* **2008**, *8*, 4488−4492.

(36) Delerue, C.; Lannoo, M.; Allan, G. *Phys. Status Solidi B* **2001**, *227*, 115−149.

(37) Sapra, S.; Shanthi, N.; Sarma, D. D. *Phys. Rev. B: Condens. Matter Mater. Phys.* **2002**, *66*, 205202.

(38) Cohen-Tannoudji, C.; Dupont-Roc, J.; Grynberg, G.; Thickstun, P. *Atom-photon interactions: basic processes and applications*; Wiley Online Library: New York, 1992.

(39) Klimov, V.; McGuire, J.; Schaller, R.; Rupasov, V. *Phys. Rev. B: Condens. Matter Mater. Phys.* **2008**, *77*, 195324.

(40) Korkusinski, M.; Voznyy, O.; Hawrylak, P. *Phys. Rev. B: Condens. Matter Mater. Phys.* **2011**, *84*, 155327.

(41) See Figure S1 in the SI for variation of Auger recombination rates with broadening.

(42) Korkusinski, M.; Zielinski, M.; Hawrylak, P. *J. Appl. Phys.* **2009**, *105*, 122406.

(43) Polizzi, E. 2012, arXiv preprint arXiv:1203.4031. (Accessed March 2016).

(44) Korkusinski, M.; Voznyy, O.; Hawrylak, P. *Phys. Rev. B: Condens. Matter Mater. Phys.* **2010**, *82*, 245304.

DOI: 10.1021/acs.nanolett.6b03059
Nano Lett. 2016, 16, 6491−6496

(45) We note that changing off-site dielectric screening from bulk dielectric constant of CdSe to that of CdS affects our results by less than 20%.
(46) Kobayashi, Y.; Nishimura, T.; Yamaguchi, H.; Tamai, N. *J. Phys. Chem. Lett.* **2011**, *2*, 1051−1055.
(47) An, J.; Franceschetti, A.; Dudiy, S.; Zunger, A. *Nano Lett.* **2006**, *6*, 2728−2735.

DOI: 10.1021/acs.nanolett.6b03059
Nano Lett. 2016, 16, 6491−6496